Mathematical modelling elucidates core mechanisms underpinning GnRH pulse generation

Margaritis Voliotis[1,2,*], Xiao Feng Li[3], Ross De Burgh[3], Geffen Lass[3], Stafford L Lightman[4], Kevin T. O'Byrne[3], Krasimira Tsaneva-Atanasova[1,2,*]
1 Department of Mathematics and Living Systems Institute, College of Engineering, Mathematics and Physical Sciences, University of Exeter, Exeter, EX4 4QF, UK
2 EPSRC Centre for Predictive Modelling in Healthcare, University of Exeter, Exeter, EX4 4QJ, UK.
3 Department of Women and Children's Health, School of Life Course Sciences, King's College London, London SE1 1UL, UK.
4 Henry Wellcome Laboratory for Integrative Neuroscience and Endocrinology, University of Bristol, Bristol, BS1 3NY, UK.

Corresponding Authors:

* M.Voliotis@exeter.ac.uk, K.Tsaneva-Atanasova@exeter.ac.uk

Keywords: gonadotrophin-releasing hormone, arcuate nucleus, kisspeptin neurones, network model, dynamical system, bifurcation analysis

Abstract (max 250 words)

Fertility critically depends on the pulsatile release of gonadotropin-releasing hormone (GnRH) from the hypothalamus. Arcuate nucleus (ARC) kisspeptin neurons, known as KNDy for co-expressing neurokinin B (NKB) and dynorphin (Dyn), are thought to comprise the core of what is known as the GnRH pulse generator. The operation of this neural construct at an appropriate ultradian frequency, is essential for gametogenesis and ovulation by driving the pulsatile release of the gonadotropic hormones LH and FSH. Although the frequency of the GnRH pulse generator is tightly controlled throughout life to maintain normal reproductive health, the underlying regulatory mechanisms remain unknown. We propose a novel mathematical model of the KNDy network and present theoretical and experimental evidence that continuous basal activity in the network initiates and maintains GnRH/LH pulsatility, and that small changes in network firing can have a large impact on pulse frequency. The model highlights that positive feedback in the population exerted by NKB and negative feedback mediated by Dyn are the two key components of the pulse generator, which operates as a relaxation oscillator. Furthermore, our model predicts the stimulatory or inhibitory response of the system to various neuropharmacological perturbations and reconciles long-standing inconsistent experimental observations following such interventions *in vivo*; a conundrum frequently associated with the gonadal steroid milieu. Our model offers insight into the modus operandi of the KNDy neural construct and the elusive mechanisms underlying GnRH pulse generation that control fertility.

Introduction

The periodic release of gonadotrophin-releasing hormone (GnRH) plays a central role in control of mammalian reproduction and is driven by hypothalamic neuronal networks (1). The operation of these networks at a frequency appropriate for the species is critical for the generation of gonadotrophin hormone signals (luteinizing hormone, LH; and follicle-stimulating hormone, FSH) by the pituitary gland, which stimulate the gonads and set in motion gametogenesis and ovulation. However, the mechanisms underlying GnRH pulse generation and frequency control remain poorly understood.

GnRH is produced from specialised neurons, known as GnRH neurones, and its secretion into the pituitary portal circulation is controlled by upstream hypothalamic signals (1). The neuropeptide kisspeptin has been identified as a key regulator of GnRH secretion as both humans and rodents with inactivating mutations in kisspeptin or its receptor fail to progress through puberty or show normal pulsatile LH secretion (2-4). Within the hypothalamus, two major kisspeptin producing neuronal populations are located in the arcuate nucleus (ARC) and in the preoptical area (5) or the anteroventral periventricular (AVPV)/rostral periventricular (PeN) continuum in rodents (6). Moreover, the invariable association between neuronal activity in the ARC and LH pulses across a range of species from rodents to primates (7) has been suggestive that the ARC is the location of the GnRH pulse generator, and therefore the ARC kisspeptin neurons, also known as KNDy for co-expressing neurokinin B (NKB) and dynorphin (Dyn) alongside kisspeptin (8), constitute the core of the GnRH pulse generator.

Although animal studies have shown that KNDy neurons are critical for the regulation of GnRH secretion, there has been relatively little information on the regulatory mechanisms involved in generating and sustaining pulsatile dynamics. Pharmacological modulators of kisspeptin, NKB and Dyn signalling have been extensively used to perturb the system and study the effect on the activity of a hypothalamic neuronal population (using ARC multiunit activity (MUA) volleys, an electrophysiological correlate of GnRH pulse generator activity, as a proxy) (9), as well as on downstream GnRH/LH pulse dynamics (10-13). For example, it has been shown that kisspeptin (Kp-10) administration does not affect MUA volleys in the ovariectomized rat (11), suggesting that kisspeptin is relaying the pulsatile signal to GnRH neurones rather than generating it. On the contrary, administration of NKB or Dyn modulates MUA volley frequency in the ovariectomized goat (13), suggesting a more active role for these neuropeptides in the generation of the pulses. Deciphering, however, the role of NKB has been problematic, and there exist conflicting data showing either an increase or decrease of LH levels in response to administration of a selective NKB receptor agonist (senktide) (10, 12, 14). Recently, a study combining optogenetics, with whole-cell electrophysiology and molecular pharmacology has shed light on the action of the neuropeptides NKB and Dyn in the KNDy network (15), with the key mechanistic finding that NKB functions as an excitatory signal by depolarising KNDy cells at the post-synaptic site, while co-released Dyn functions pre-synaptically to inhibit NKB release.

Using a combination of theoretical and experimental work, we aim to shed light on the mechanisms generating and modulating GnRH/LH pulsatile dynamics. Motivated by the experimental findings described above, we developed a mathematical model of the ARC KNDy network. The model predicts that the KNDy population behaves as a relaxation oscillator: autonomously generating and sustaining oscillatory firing dynamics similar to the hypothalamic MUA volleys observed *in vivo* (9, 10). Furthermore, critical for GnRH pulsatile dynamics is *continuous* basal activity within the ARC KNDy population. We tested this prediction *in vivo* using optogenetics and showed that low-frequency *continuous* neuronal activation in the ARC KNDy network initiates GnRH/LH pulsatility in female estrous mice and small changes in basal network firing can have a large impact on pulse frequency. Finally, our model predicts the response of the system to various neuropharmacological perturbations and reconciles inconsistent experimental observations following such interventions *in vivo*.

Results

The ARC KNDy population network model.

We propose a mathematical network model (Fig. 1A) to describe and study the collective dynamics of ARC KNDy neurons. The model describes the dynamics of M synaptically connected KNDy neurons using a set of coupled ordinary differential equations (ODEs). For each neuron i, we use variables D_i and N_i, to denote the concentration of Dyn and NKB, secreted at its synaptic ends; and variable v_i to denote its firing rate, measured in spikes/min. The dynamics of neuron i in the population are given by:

$$\frac{dD_i}{dt} = f_D(v_i) - d_D D_i; \qquad [1]$$

$$\frac{dN_i}{dt} = f_N(v_i, D_i) - d_N N_i; \qquad [2]$$

$$\frac{dv_i}{dt} = f_v([v_j, N_j]_{j \in \mathrm{neigh}(i)}) - d_v v_i. \qquad [3]$$

Parameters d_D, d_N and d_v mostly govern the characteristic timescale for each variable. In particular, parameters d_D and d_N correspond to the rate at which Dyn and NKB are lost (e.g. due to diffusion or active degradation), while d_v relates to the rate at which neuronal activity resets to its basal level. Functions f_D, f_N give the secretion rate of Dyn and NKB, respectively, while function f_v encodes how the firing rate changes in response to synaptic inputs. Crucially, the activity of neuron i, v_i, depends on the firing rate and secreted level of NKB of all other neurons j that are synaptically connected to it. This dependence is denoted by the square brackets notation in the arguments list of f_v. Synaptic connections are summarised by the adjacency matrix, A: a binary, square ($M \times M$) matrix with $A_{ij} = 1(0)$ indicating synaptic connectivity from neuron i to neuron j. In the model, synaptic connections are formed randomly between all neurons with a constant probability, i.e., $\mathrm{Prob}(A_{ij} = 1) = \bar{c}$.

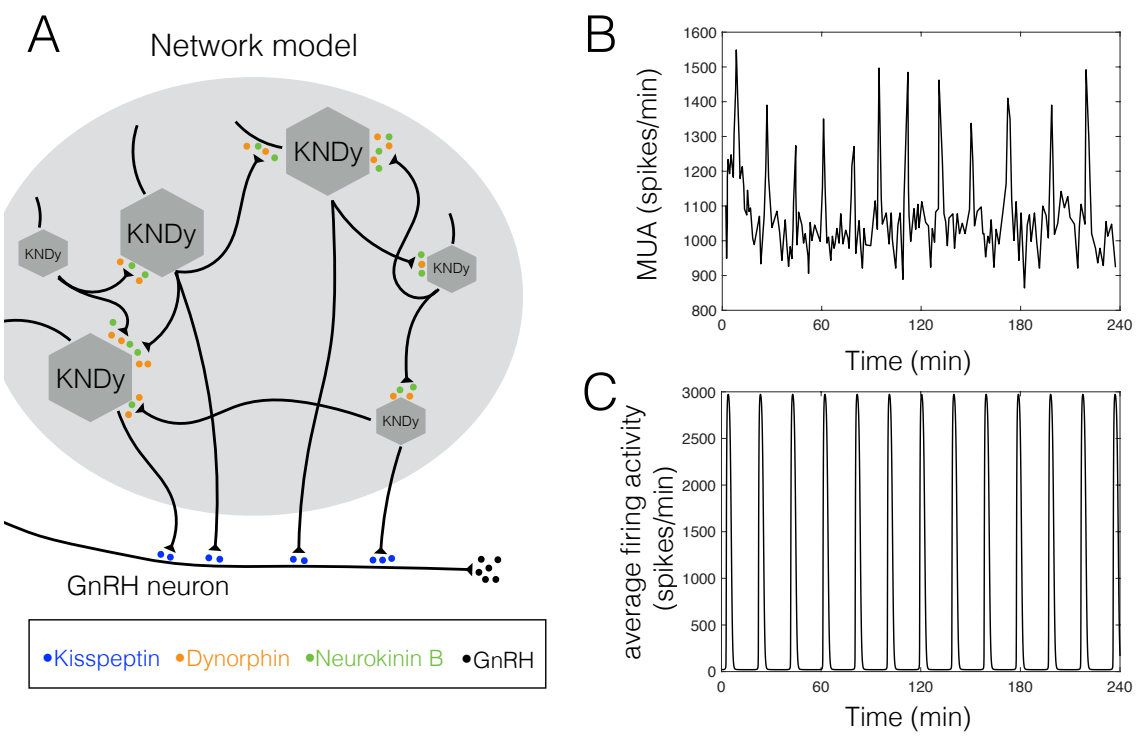

Figure 1: **A network model of KNDy neurons in the arcuate nucleus (ARC).** (A) Schematic illustration of the dynamical, network model comprising a population of synaptically connected KNDy neurons. In the model, the neuronal firing rate drives the secretion of regulatory neuropeptides dynorphin (Dyn) and neurokinin B (NKB). Furthermore, NKB excites postsynaptic neurons while Dyn inhibits NKB secretion pre-synaptically. (B) Multi-unit activity (MUA) volleys recorded from the hypothalamus of an ovariectomized rat (data from (10)). (C) The model produces sustained oscillations with explosive spikes of neuronal activity similar to those observed *in vivo*. Model parameters were inferred from the data in (B) using an Approximate Bayesian Computation method based on sequential Monte Carlo (ABC SMC; see Material and Methods section) and are listed in Table 1.

We employ the following sigmoidal (Hill-type) functions to describe regulatory relationships between the variables. In particular, we set the secretion rate of Dyn and NKB to be:

$$f_D(v) = k_D \frac{v^{n_1}}{v^{n_1} + K_{v,1}^{n_1}};$$

$$f_N(v, D) = k_N \frac{v^{n_2}}{v^{n_2} + K_{v,2}^{n_2}} \frac{K_D^{n_3}}{D^{n_3} + K_D^{n_3}}.$$

That is, neuronal activity stimulates secretion of both neuropeptides, and Dyn represses NKB secretion (15). The rate of neuropeptide release is inherently limited by the diffusion of cytoplasmic secretory vesicles (16), therefore in the model we allow saturation of the secretion rates via parameters $K_{v,1}$, $K_{v,2}$ and K_D. Furthermore, we set:

$$f_v\left([v_j, N_j]_{j\in\text{neigh}(i)}\right) = v_0 \left(\frac{2}{\exp(-I) + 1} - 1\right);$$

$$I = I_0 + \sum_{j\in\text{neigh}(i)} p_v \frac{N_j^{n_4}}{N_j^{n_4} + K_N^{n_4}} v_j,$$

where v_0 is the maximum rate at which the firing rate increases in response to synaptic inputs. The stimulatory effect of NKB (secreted at the presynaptic end) is mediated via G protein-coupled receptor Tacr3 and is manifested as a short-term depolarisation of the postsynaptic neuron (15). In the equation above, we accommodate this effect by letting the synaptic strength be a function of the secreted NKB. Moreover, parameter p_v sets the maximum strength of the synapse, while parameter K_N sets the level of NKB at which its effect is half-maximal. Finally, parameter I_0 controls the basal neuronal activity in the population, which could stem from synaptic noise or synaptic inputs.

We infer model parameters using the frequency and duty-cycle of the MUA volleys recorded from the hypothalamus of ovariectomized rats (10) (see Material and Methods section). As illustrated in Fig. 1B&C, the model can replicate pulses of synchronised activity similar to the MUA signal recorded *in vivo*. This finding further supports the hypothesis that KNDy neurons in the ARC constitute the core of the GnRH pulse generator.

Analysis of the model reveals the KNDy population functions as relaxation oscillator.

Having shown that the model can reproduce sustained pulses of neuronal activity (see Fig. 1B), we proceed to study the mechanisms driving the phenomenon. To do so we derive a coarse-grained (mean-field) model of the neuronal population dynamics comprising three dynamical variables: $\overline{D}$, representing the average concentration of Dyn secreted; $\overline{N}$, representing the concentration of NKB secreted; and $\bar{v}$, representing the average firing activity of the neuronal population. Derivation of the coarse-grained model proceeds by averaging Eqn. [3] over all neurons (index *i*); and expanding (keeping up to leading term) all non-linear functions of D_i , N_i, and v_i around the population-averaged values, $\overline{D} = \sum_i D_i/M$, $\overline{N} = \sum_i N_i/M$and $\bar{v} = \sum_i v_i/M$ (see S1 text). The resulting equations, describing the time evolution of the population-averaged variables, are:

$$\frac{d\overline{D}}{dt} = f_D(\bar{v}) - d_D\overline{D}; \quad [4]$$

$$\frac{d\overline{N}}{dt} = f_N(\bar{v}, \overline{D}) - d_N\overline{N}; \quad [5]$$

$$\frac{dv_i}{dt} = f_v(\bar{v}, \overline{N}) - d_v\bar{v}. \quad [6]$$

All parameters and functions are defined as before (see section above), except for synaptic input I that now takes the form: $I = I_0 + p_v\bar{c}M\frac{N^{n_4}}{N^{n_4}+K_N^{n_4}}\bar{v}$, where $\bar{c}$ is the average number of synapses that a neuron receives as a fraction of the population size.

To investigate the role of Dyn-mediated negative feedback in the model dynamics we perform fast – slow analysis (17) of the coarse-grained model Eqns. [4–6]. In our model $\overline{D}$ changes on slower time-scale compared to the other two variables. This allows us to study the dynamics of the fast subsystem, comprised of $\overline{N}$ and $\bar{v}$, as a function of the slow variable, $\overline{D}$, which is treated as a constant (bifurcation) parameter. The result of this analysis is illustrated in Fig. 2B and shows that for intermediate values of Dyn the fast subsystem describing the dynamics of $\overline{N}$ and $\bar{v}$ is bi-stable as demonstrated by the co-existing high and low branches of stable equilibria shown in Fig. 2B. This bi-stable behaviour, stemming from the non-linear, positive feedback between neuronal activity and NKB secretion, leads to sustained oscillations of neuronal activity when combined with slow negative feedback mediated through Dyn.

Next, in order to investigate the role of basal neuronal activity within the KNDy network in the generation and modulation of oscillatory activity in the network (note that we now consider the full system given by Eqns. [4–6]), we treat parameter I_0 as a bifurcation parameter. We find that oscillatory behavior of the system is possible within a critical range of intermediate values of I_0. In particular, as I_0 is increased from zero, high-amplitude, low-frequency pulses emerge via a homoclinic bifurcation (Fig. 2C; HC point). The threshold value of I_0 at which the bifurcation occurs is equivalent to driving the neuronal population at a rate of approximately 0.024 Hz in the absence of NKB and Dyn modulation. As external excitation ramps up, the frequency of pulses continues to increase, until oscillations disappear altogether via a Hopf bifurcation (Fig. 2C; HB point) and the system re-enters a silent (non-oscillatory) regime.

In engineering terms, the system behaves as a relaxation oscillator, where the bi-stable subsystem is successively triggered by external excitation and silenced due to negative feedback. We should note that a sufficiently slow negative feedback can sustain oscillations in the absence of bi-stability, however, we also note that the combination of bi-stability and negative feedback is a recurring motif in many biological oscillators (18).

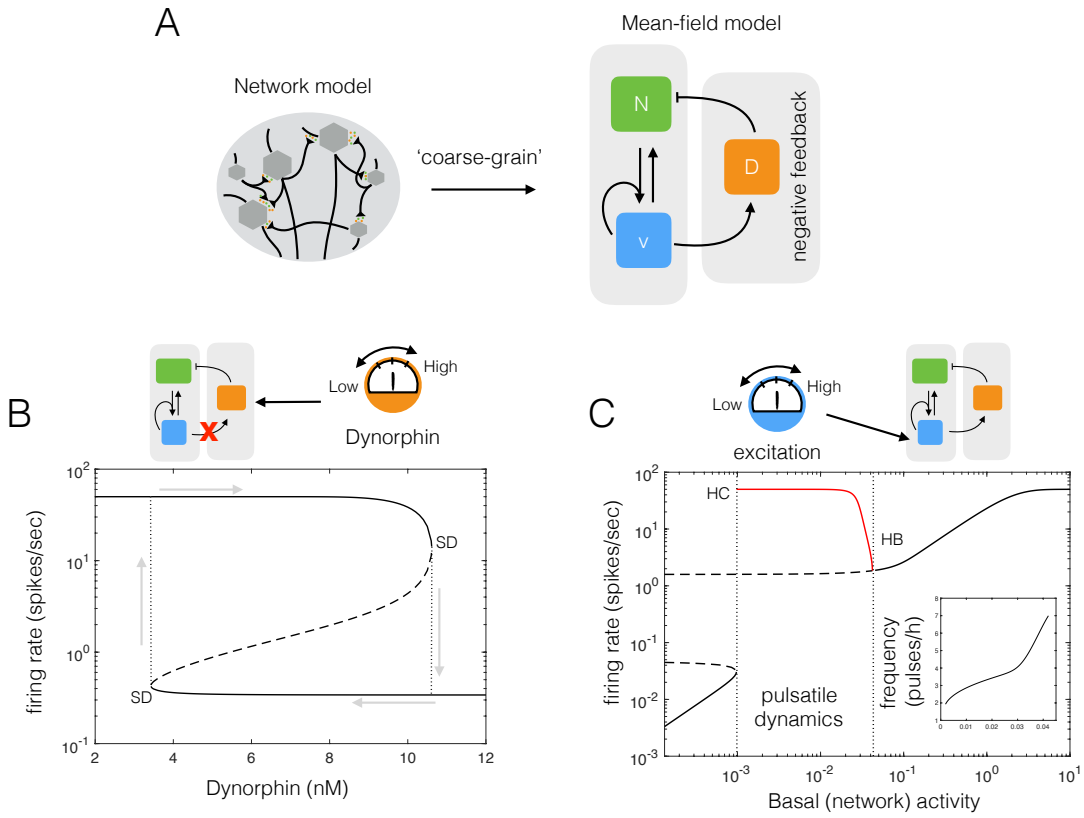

Figure 2: **A coarse-grained model gives mechanistic insight into the pulsatile behavior of the neuronal population.** (A) We reduce the network model by deriving a mean-field model of the neuronal population comprising three dynamical variables: $\overline{D}$, representing the average concentration of Dyn secreted; $\overline{N}$, representing the concentration of NKB secreted; and $\bar{v}$, representing the average firing activity of the neuronal population. (B) After disrupting the negative feedback loop (i.e., setting Dynorphin under external control) the system exhibits, for intermediate values of Dynorphin, two stable equilibria (upper and lower solid lines) and an unstable one (dashed line). At the edges of the bi-stable regime equilibria are lost through a saddle-node bifurcation (SD points). The bi-stability gives rise to hysteresis as the value of Dyn is varied externally (grey arrows). (C) The coarse-grained model predicts how basal neuronal activity affects the system's dynamics and pulse frequency. As basal activity is increased from zero, high-amplitude, low-frequency pulses emerge after some critical value (HC point; homoclinic bifurcation). The frequency of pulses continues to increase with increase in basal activity until oscillations disappear altogether (HB point; Hopf bifurcation) and the system enters a mono-stable regime. Model parameter values are given in Table 1.

Continuous optogenetic activation of KNDy neurons generates pulsatile LH secretion *in vivo*.

To test the model predictions that continuous excitatory signals can trigger pulsatility and increase pulse frequency, we stimulated the KNDy neural system in Kiss-Cre mice (19) using optogenetics. ARC kisspeptin-expressing neurons were transduced with a Cre-dependent adeno-associated virus (AAV9-EF1-dflox-hChR2-(H134R)-mCherry-WPRE-hGH) to express channelrhodopsin (ChR2). AAV-injected, Kiss-Cre mice were implanted with a fiber optic cannula in the ARC and the effects on LH pulsatility of continuous stimulation at different frequencies was tested. After 1 h of controlled blood sampling, low-frequency optic stimulation, 5-ms pulses of blue light (473 nm) at 0.5, 1 or 5 Hz, was initiated and continuously delivered for 90 min. Control mice received no optic stimulation. During the course of the experiment, blood samples (5μl) were collected every 5 min. To maximise the effect of optogenetic stimulation, estrous mice were used which display the minimum intrinsic pulse generator frequency (20). Indeed, the majority of the control non-optically stimulated Kiss-Cre mice in estrus exhibited no LH pulse or intermittently 1 pulse during the 2.5 h sampling period (Fig. 3, B, F). Similarly,

no LH pulses or occasionally 1 LH pulse was observed in the 60 min control period in the optically stimulated mice. Optic stimulation at 0.5 Hz failed to induce LH pulses (Fig. 3, C, F). In line with theoretical predictions increasing the low-frequency continuous stimulation to 1 Hz evoked regular LH pulses (Fig. 3, D, F), while 5 Hz increased LH pulse frequency further. Importantly we show that the observed increase in LH pulse frequency *in vivo* was statistically significant ($p < 0.05$) (Fig. 3, F). Continuous optogenetic stimulation (5 Hz) of AAV-injected wild-type C57BL/6 estrous mice (n = 3) failed to induce LH pulses (data not shown).

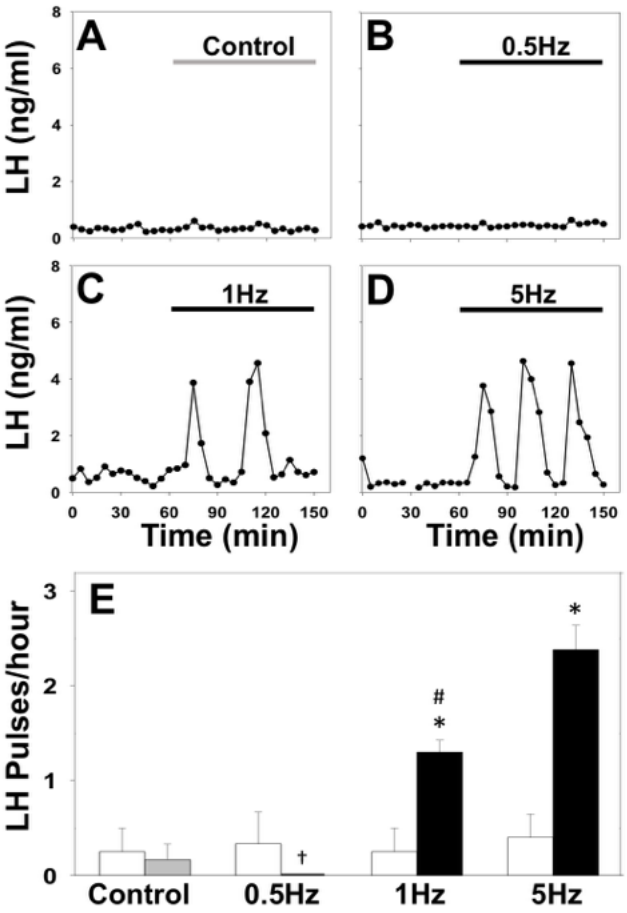

Figure 3: **Effect of optogenetic stimulation of ARC kisspeptin neurons on LH pulse frequency in estrous Kiss-Cre mice**. (A) ARC kisspeptin neurons transfected with ChR2. Photomicrographs showing ChR2-mCherry immunofluorescence in the ARN in the slice preparation. Blue arrow shows the track of an optical fiber above ARC kisspeptin neurons expressing ChR2. 3V, third ventricle; ARN, the arcuate nucleus, (Scale bar, 300μm). (B-E) Representative examples showing LH secretion in response to no stimulation (grey bar) as control (B), or continuous blue light (473 nm, 5-ms pulse width, black bar) activation of kisspeptin neurons at 0.5 Hz (C), 1 Hz (D) or 5 Hz (E). (F) Summary showing mean ± SEM changes in LH pulse frequency. *$P < 0.05$ vs pre-stimulation; $^{\#}P < 0.05$ vs stimulation at same time point. † Absence of LH pulses in response to 0.5 Hz stimulation. n = 4-6 per group.

Further Physiological Implications of the Analysis.

Our model also predicts the response of the system to various neuropharmacological perturbations and reconciles inconsistent experimental observations following such interventions *in vivo*. Neuropharmacology is a powerful tool used to study the role of neurotransmitter and neuropeptide

signalling on the pulsatile GnRH dynamics. *In vivo*, localized administration of drugs that selectively activate or inhibit certain pathways of interest, can shed light on the regulatory mechanism underlying pulse generation and frequency modulation. However, the effect of such neuropharmacological perturbations can appear confusing and difficult to interpret when feedback interactions and non-linearities are present in the system. One notable example, regards senktide (a selective NKB receptor agonist) that appears to be suppressing pulsatile GnRH/LH dynamics in some cases (10, 14) while stimulating LH secretion in others (12). To investigate this controversial finding, we extend our coarse-grained model to accommodate the effect of two drugs often used to perturb the system *in vivo*: senktide, a selective NKB receptor agonist; and nor-BNI, a selective κ-opioid receptor antagonist. We use E to denote the drug concentration injected into the system. As senktide has the same effect as NKB but functions independently, we incorporate it in our model by modifying the expression for the synaptic input I as follows:

$$I = I_0 + p_v \bar{c} M \frac{N^{n_4} + E^{n_4}}{N^{n_4} + E^{n_4} + K_N^{n_4}} \bar{v}$$

On the other hand, nor-BNI blocks Dyn signalling, therefore we modify function $f_N(v, D)$ to read:

$$f_N(v, D) = k_N \frac{v^{n_2}}{v^{n_2} + K_{v,2}^{n_2}} \frac{K_D^{n_3} + E^{n_3}}{D^{n_3} + E^{n_3} + K_D^{n_3}}$$

That is, the antagonist is effectively increasing parameter $K_{v,2}$ in the model.

Figure 4 A&B illustrates that the effect of perturbing the system with senktide varies depending on the underlying NKB and Dyn secretion capacity (parameters k_N and k_D in the model). In particular, Fig. 4A shows the region over the parameter space (grey area) for which the unperturbed system demonstrates pulsatile dynamics. This region is deformed after senktide administration, and given the system starts from within the oscillatory regime three distinct response types are observed (see Fig. 4B; indicative examples are marked with numbers). First, administration of senktide can set the system in a steady-state of elevated activity after a transient spike (see trace marked 1). Such an effect is consistent with data from diestrous rats, showing that intracerebroventricular administration of senktide to gonadal intact rats in diestrus stimulated transient LH secretion (10). Second, administration of senktide can increase the pulse frequency (see trace marked 2 and Fig. C in S1 text). This type of response is consistent with data showing that intracerebroventricular administration of NKB increases the frequency of multiunit electrical activity (MUA) volleys recorded from the medial basal hypothalamus in the ovariectomized goat (13). An increase in the frequency of MUA volleys in response to central nor-BNI administration (13) is also in agreement with the model (see Fig. B in S1 text). Finally, administration of senktide can suppress pulsatile dynamics setting the system in a low activity equilibrium state (see trace marked 3). This apparent inhibition of the system through an excitatory agent although counter intuitive is in agreement with the inhibition of hypothalamic MUA volleys and serum LH observed in adult ovariectomized rats after intracerebroventricular administration of senktide (10). Fig. 4C illustrates the effect of perturbing the system with a combination of NKB and nor-BNI. Note, that the combined administration of the two drugs can preserve pulsatile dynamics in cases where senktide alone was suppressing it (see trace 3); in agreement with experimental data showing that nor-BNI blocks the senktide-induced suppression of pulsatile LH secretion in OVX rats (10).

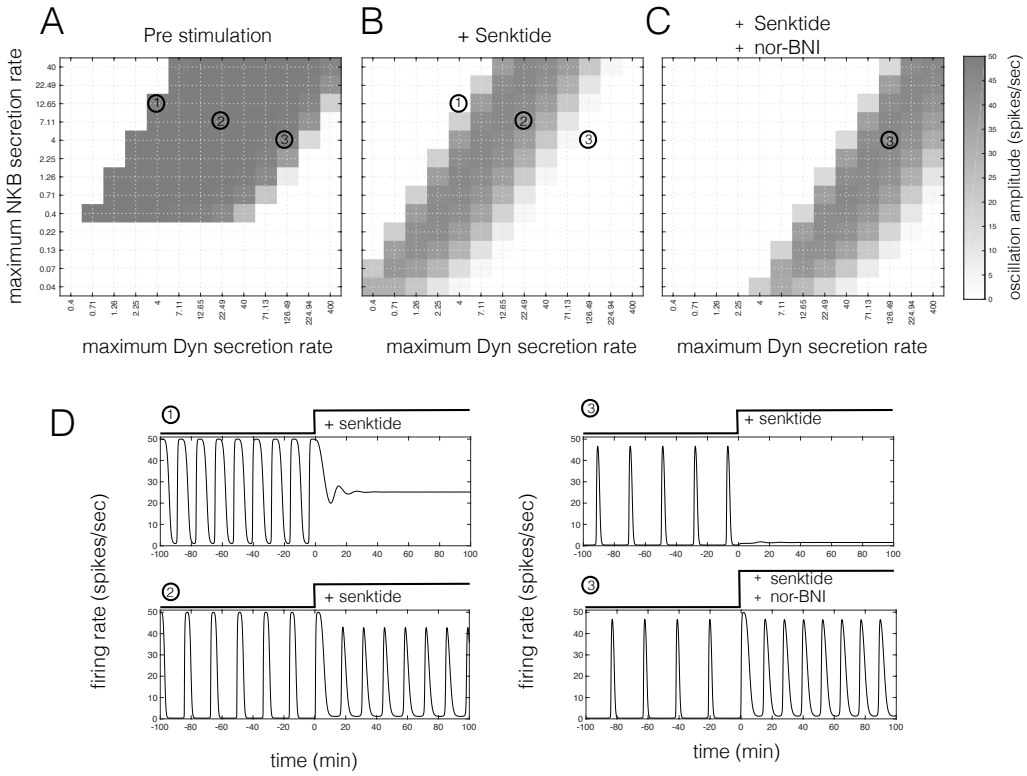

Figure 4: **The effect of neuropharmacological perturbations on the activity of the KNDy population.** Perturbation of the system with two drugs: senktide, a selective NKB receptor agonist; and nor-BNI, a selective Dyn receptor antagonist. The effect of the perturbation on the dynamics depends on the NKB and Dyn secretion rate. (A) The magnitude of oscillations (grey scale) in the unperturbed system for different levels of maximum NKB and Dyn secretion rate (parameters k_N and k_D in the model). (B) The magnitude of oscillations after perturbing the system with senktide ($E_{senktide} = 60$ pM). (C) The magnitude of oscillations after perturbing the system with senktide ($E_{senktide} = 60$ pM) and nor-BNI ($E_{nor-BNI} = 4.1$ nM) simultaneously. (D) Time-traces of the system activity in response to neuropharmacological perturbations with senktide and nor-BNI. Time-traces correspond to the (k_N, k_D) combinations marked in (A)-(C).

Discussion

Motivated by recent experimental evidence, we developed and studied a mathematical model of the KNDy population in the ARC, a population proposed to comprise the core of the GnRH pulse generator (21, 22). Our model demonstrates that the KNDy population can indeed produce and sustain pulsatile dynamics working as a relaxation oscillator. On the one hand, basal neuronal activity and auto-stimulation via NKB signalling allows the population to behave as a bi-stable switch, firing either at a high or low rate. Moreover, negative feedback through Dyn signalling allows the population to switch between the two activity states in a regular manner, giving rise to pulses of neuronal activity. Using global sensitivity analysis, we found that this mechanism of pulse generation is robust to parameter perturbations (see S1 text). In fact, co-variation of parameters governing, for example, the magnitude of basal activity, and the maximum secretion rates of NKB and Dyn is a more effective way of modulating the systems' oscillatory behaviour (amplitude and frequency). This multi-channel mode of efficient regulation is perhaps not surprising given the system's crucial function, and hints that steroid feedback modulating the dynamics of the pulse generator over the reproductive cycle in female mammals is mediated through multiple, possibly interlinked, pathways.

Following model predictions, we explored the effect of continuous optogenetic activation of the KNDy population on LH pulse dynamics. The model predicts that pulsatile dynamics of the system critically

depend on the levels of basal activity of the KNDy population. For example, starting from a silent or low frequency state of the system, increasing levels of basal activity can reinstate pulsatile dynamics or increase the frequency. Using an experimental protocol suggested by the model analysis we have tested these model predictions *in vivo* using optogenetics (22-24), and showed that we are able to directly control the generation and frequency of LH pulses in estrous mice by selectively exciting KNDy neurons in a continuous fashion at 1Hz and 5Hz. It is important to note that the model has informed the design of the experiments by suggesting the use of low-frequency optic stimulation for the first time in investigating LH pulse generation and in contrast to previous studies (22-24). Our results suggest that inhibitory or excitatory synaptic signalling within the KNDy neural population have a drastic effect on GnRH/LH pulse dynamics. We speculate that this enables KNDy neurons to integrate and transmit information regarding the overall state of the organism that is relevant for reproduction: for example, information on the emotional state and stress level through synaptic connections originating at the level of the amygdala (25), a key limbic brain structure; or information regarding the nutritional state of the organism through connections from Agouti-related peptide (AgRP)-expressing neurons in the hypothalamus (26).

The proposed model allowed us to study the effect of pharmacological modulators of NKB and Dyn signalling. We find that NKB receptor agonists, such as senktide, could have either an inhibitory or an excitatory effect on the dynamics of the model. We show that this response variability can be explained, for example, by variation in parameters that control the levels of Dyn and NKB secreted by the neurons, which *in vivo* are controlled by the sex-steroid milieu. This finding reconciles previous conflicting evidence regarding the effect of senktide on the levels of LH secretion (10, 12, 14). Our results also highlight the need for a quantitative understanding of how the sex-steroid milieu affects the NKB and Dyn signalling pathways in the KNDy population. Such an understanding will lead to more accurate interpretation of results from *in vivo* neuropharmacological perturbation experiments in various animal models and will shed light on the mechanisms underlying the regulation of LH pulsatile secretion. We envision that as hormonal measurement techniques advance, enabling accurate, real-time readouts from individuals at low cost, such predictive mathematical models would be a valuable tool for understanding of reproductive physiopathology from puberty to menopause.

Materials and methods

Bifurcation analysis and numerical experiments

Bifurcation analysis of the coarse-grained model was performed using AUTO-07p (27). Both the full network model and coarse-grained model were simulated in Matlab using function ode45 (explicit Runge-Kutta (4, 5) solver).

Parameter inference

Parameter inference was performed using an Approximate Bayesian Computation (ABC) method based on sequential Monte Carlo (SMC) (28). In ABC SMC a population of parameter vectors or particles, θ, is initially sampled form the prior distribution π_0 and propagated with the use of a perturbation kernel through a sequence of distributions $\pi_i, i = 1, \dots, \mathcal{T}$. The final distribution $\pi_{\mathcal{T}}(\theta | d(x, x^*) < \epsilon_{\mathcal{T}})$ corresponds to the (approximate) target posterior distribution, where $d(x, x^*)$ is the distance function comparing the simulated dataset x^* to the experimental data x and $\epsilon_{\mathcal{T}}$ is the final error tolerance level. Intermediate distributions are associated with a series of decreasing tolerance levels $\epsilon_i, i = 1, \dots, \mathcal{T} - 1$, making the transition to $\pi_{\mathcal{T}}$ more gradual and avoiding getting stuck in areas of low probability.

Here, to ensure gradual transition between populations we take $\mathcal{T} = 4$ and set tolerance levels to $\epsilon_i = 10^{(2-i)}, i = 1, \dots, \mathcal{T}$. The size of each population is set to 500 particles. For each particle, the activity of the KNDy is simulated from $t = 0$ to 6000 min, the first 1000 min are discarded, and the remaining time-trace is used to calculate the pulse frequency and duty cycle (defined as the fraction of one period in which KNDy activity is above 50% of the pulse amplitude). The distance function, d, is defined as the sum of the squared relative error in these two summary statistics between the simulated dataset and the data (see Fig. 1A; frequency 3.12 pulses/hour; duty cycle 0.15). The prior parameter distributions were chosen as follows: $\log_{10}(d_D) \sim \mathcal{U}(-2,1)$; $\log_{10}(d_N) \sim \mathcal{U}(-2,1)$; $\log_{10}(d_v) \sim \mathcal{U}(0,2)$; $\log_{10}(k_D) \sim \mathcal{U}(-1,3)$; $k_N \sim \mathcal{N}(40,4)$ estimate from (29) plus 10% error; $\log_{10}(p_v) \sim \mathcal{U}(-3,1)$; $K_D \sim \mathcal{N}(0.3,0.03)$ estimate from (30) plus 10% error; $K_N \sim \mathcal{N}(4,0.4)$ estimate from (31) plus 10% error; $K_{v,1} \sim \mathcal{U}(1,3)$; $K_{v,2} \sim \mathcal{U}(1,3)$; $\log_{10}(I_0) \sim \mathcal{U}(-3,0)$, where $\mathcal{U}(min, max)$ denotes the uniform distribution in the interval $[min, max]$, and $\mathcal{N}(\mu, \sigma)$ denotes the normal distribution with mean, μ, and standard deviation, σ. For parameters k_N, K_D, K_N, $K_{v,1}$, and $K_{v,2}$ gaussian perturbation kernels were used with standard deviation 4, 0.03, 0.4, 10 and 10 respectively. For all remaining parameter log-normal perturbation kernels were used with standard deviation 0.05. An (approximate) maximum a posteriori (MAP) estimate of model parameters (corresponding to the parameter values of the most probable particle in the final population) is given in Table 1. Histograms of the approximate marginal posterior distribution of each parameter and pairwise scatter plots are shown in Fig. A in S1 text.

Animals

Breeding pairs of Kiss-Cre heterozygous transgenic mice (32) were obtained from the Department of Physiology, Development and Neuroscience, University of Cambridge, UK. Litters from the breeding pairs were genotyped by polymerase chain reaction (PCR) analysis. Adult female mice (8-14 wk old; 25-30g) heterozygous for the Kiss-Cre transgene or wild-type C57BL/6 littermates, with normal pubertal development and estrous cyclicity, were used. Mice were housed under a 12:12 h light/dark cycle (lights on 0700 h) at 22 ± 2 °C and provided with food (standard maintenance diet; Special Dietary Services, Wittam, UK) and water ad libitum. All animal procedures performed were approved by the Animal Welfare and Ethical Review Body (AWERB) Committee at King's College London, and in accordance with the UK Home Office Regulations.

Surgical procedures

Surgical procedures for stereotaxic injection of AAV9-EF1-dflox-hChR2-(H134R)-mCherry-WPRE-hGH (4.35 x 1013 GC/ml; Penn Vector Core) to express channelrhodopsin (ChR2) in ARC kisspeptin neurons were performed under aseptic conditions with general anaesthesia induced by ketamine (Vetalar, 100 mg/kg, i.p.; Pfizer, Sandwich, UK) and xylazine (Rompun, 10 mg/kg, i.p.; Bayer, Leverkusen, Germany). Kiss-Cre female mice (n = 7) or wide-type (n = 3) were secured in a David Kopf Motorized stereotaxic frame and surgical procedures were performed using a Robot Stereotaxy system (Neurostar, Tubingen, Germany). A small hole was drilled into the skull at a location above the ARC. The stereotaxic injection coordinates used to target the ARC were obtained from the mouse brain atlas of Paxinos and Franklin (33) (0.3 mm lateral, 1.2 mm posterior to bregma and at a depth of 6.0 mm). Using a 2-μL Hamilton micro-syringe (Esslab, Essex, UK) attached to the Robot Stereotaxy, 1 μl of the AAV-construct was injected unilaterally into the ARC at a rate of 100 nl/min. The needle was left in position for a further 5 min and then removed slowly over 1 min. A fibre optic cannula (200 μm, 0.39NA, 1.25mm ceramic ferrule; Thorlabs LTD, Ely, UK) was then inserted at the same co-ordinates as the injection site, but to a depth of 5.88 mm, so that the fibre optic cannula was situated immediately above the latter. Dental cement or a glue composite was then used to fix the cannula in place, and the skin incision closed with suture. After surgery, mice were left for 4 weeks to achieve effective opsin expression. After a 1-

wk recovery period, the mice were handles daily to acclimatise them to the tail-tip blood sampling procedure (34).

Blood samplings for LH measurement

Prior to optogenetic stimulation, the very tip of the mouse's tail was excised using a sterile scalpel for subsequent blood sample collection (20). The chronically implanted fibre optic cannula was then attached via a ceramic mating sleeve to a multimode fibre optic rotary joint patch cables (Thorlabs), allowing freedom of movement of the animal, for delivery of blue light (473 nm wavelength) using a Grass SD9B stimulator controlled DPSS laser (Laserglow Technologies, Toronto, Canada). Laser intensity at the tip of the fibre optic patch cable was 5 mW. After 1 h acclimatisation, blood samples (5µl) were collected every 5 min for 2.5 h. After 1 h controlled blood sampling, continuous optic stimulation (5-ms pulse width) was initiated at 0.5, 1 or 5 Hz for 90 min. Controls received no optic stimulation. Kiss-Cre mice received the stimulation protocols in random order. Wild-type received 5 Hz optic stimulation only.

The blood samples were processed by ELISA as reported previously (34). Mouse LH standard and antibody were purchased from Harbour-UCLA, USA, and secondary antibody (NA934) was from VWR International, UK. The intra-assay and inter-assay variations were 4.6% and 10.2%, respectively.

Validation of AAV injection site

After completion of experiments, mice were anaesthetised with a lethal dose of ketamine and transcardially perfused with heparinised saline for 5 min, followed by 10 min of ice-cold 4% paraformaldehyde (PFA) in phosphate buffer (pH 7.4) for 15 min using a pump (Minipuls, Gilson, Villiers Le Bel, France). Brains were rapidly collected and postfixed sequentially at 4 °C in 15% sucrose in 4% PFA and in 30% sucrose in phosphate-buffered saline until they sank. Afterwards, brains were snap-frozen on dry ice and stored at -80 °C until processing. Brains were coronally sectioned (40-µm) using a cryostat (Bright Instrument Co., Luton, UK) and every third section was collected between -1.34 mm to -2.70 mm from the bregma. Sections were mounted on microscope slides, air-dried and cover slipped with ProLong Antifade mounting medium (Molecular Probes, Inc. OR, USA). The injection site was verified and evaluated using Axioskop 2 Plus microscope equipped with axiovision, version 4.7 (Zeiss). One of 7 Kiss-Cre mice failed to show mCherry fluorescence in the ARC and was excluded from the analysis.

LH Pulses and Statistical Analysis

Detection of LH pulses was established by use of the Dynpeak algorithm (35). The effect of optogenetic stimulation on parameters of LH secretion was calculated by comparing the mean number of LH pulse per hour, within the 90 min stimulation period with the 60 min pre-stimulation control period. For the non-stimulated control animals, the same timepoints were compared. The mean number of LH pulse per hour, within the 90 min stimulation period, or equivalent, was also compared between experimental groups. Statistical significance was testes using one-way ANOVA followed by Dunnett's test. $P < 0.05$ was considered statistically significant. Data are presented as the mean ± SEM.

Supporting information

S1 text.

Supporting Information.

Acknowledgments

KTA and MV gratefully acknowledge the financial support of the EPSRC via grant EP/N014391/1.
KOB and SLL gratefully acknowledge the financial support of the MRC via grant MR/N022637/1.

References

1. Herbison AE (2016) Control of puberty onset and fertility by gonadotropin-releasing hormone neurons. *Nature Reviews Endocrinology* 12(8):452-466.
2. de Roux N, *et al*. (2003) Hypogonadotropic hypogonadism due to loss of function of the KiSS1-derived peptide receptor GPR54. *Proceedings of the National Academy of Sciences* 100(19):10972-10976.
3. Kaiser UB (2015) Understanding reproductive endocrine disorders. *Nature Reviews Endocrinology* 11(11):640-641.
4. Seminara SB, *et al*. (2003) The GPR54Gene as a Regulator of Puberty. *New England Journal of Medicine* 349(17):1614-1627.
5. Hrabovszky E (2014) Neuroanatomy of the Human Hypothalamic Kisspeptin System. *Neuroendocrinology* 99(1):33-48.
6. Clarkson J, Danglemont de Tassigny X, Colledge WH, Caraty A, & Herbison AE (2009) Distribution of Kisspeptin Neurones in the Adult Female Mouse Brain. *Journal of Neuroendocrinology* 21(8):673-682.
7. Plant TM & Zeleznik AJ (2014) *Knobil and Neill's physiology of reproduction* (Academic Press).
8. Lehman MN, Coolen LM, & Goodman RL (2011) Minireview: Kisspeptin/Neurokinin B/Dynorphin (KNDy) Cells of the Arcuate Nucleus: A Central Node in the Control of Gonadotropin-Releasing Hormone Secretion. *Endocrinology* 151(8):3479-89.
9. Wilson RC, *et al*. (1984) Central electrophysiologic correlates of pulsatile luteinizing hormone secretion in the rhesus monkey. *Neuroendocrinology* 39(3):256-260.
10. Kinsey-Jones JS, *et al*. (2011) The Inhibitory Effects of Neurokinin B on GnRH Pulse Generator Frequency in the Female Rat. *Endocrinology* 153(1):307-315.
11. Kinsey-Jones JS, Li XF, Luckman SM, & O'Byrne KT (2008) Effects of Kisspeptin-10 on the Electrophysiological Manifestation of Gonadotropin-Releasing Hormone Pulse Generator Activity in the Female Rat. *Endocrinology* 149(3):1004-1008.
12. Navarro VM, *et al*. (2009) Regulation of Gonadotropin-Releasing Hormone Secretion by Kisspeptin/Dynorphin/Neurokinin B Neurons in the Arcuate Nucleus of the Mouse. *The Journal of Neuroscience* 29(38):11859-11866.
13. Wakabayashi Y, *et al*. (2010) Neurokinin B and Dynorphin A in Kisspeptin Neurons of the Arcuate Nucleus Participate in Generation of Periodic Oscillation of Neural Activity Driving Pulsatile Gonadotropin-Releasing Hormone Secretion in the Goat. *The Journal of Neuroscience* 30(8):3124-3132.
14. Sandoval-Guzmán T & E Rance N (2004) Central injection of senktide, an NK3 receptor agonist, or neuropeptide Y inhibits LH secretion and induces different patterns of Fos expression in the rat hypothalamus. *Brain research* 1026(2):307-312.
15. Qiu J, *et al*. (2016) High-frequency stimulation-induced peptide release synchronizes arcuate kisspeptin neurons and excites GnRH neurons. *eLife* 5:e16246-e16246.
16. Han W, Ng Y-K, Axelrod D, & Levitan ES (1999) Neuropeptide release by efficient recruitment of diffusing cytoplasmic secretory vesicles. *Proceedings of the National Academy of Sciences* 96(25):14577-14582.
17. Rinzel J (1985) Bursting oscillations in an excitable membrane model. *Ordinary and partial differential equations*, (Springer), pp 304-316.

18. Pomerening JR, Sontag ED, & Ferrell JE (2003) Building a cell cycle oscillator: hysteresis and bistability in the activation of Cdc2. *Nature Cell Biology* 5(4):346-351.
19. Adekunbi D, *et al*. (2018) Kisspeptin neurones in the posterodorsal medial amygdala modulate sexual partner preference and anxiety in male mice. *Journal of neuroendocrinology* 30(3):e12572.
20. Czieselsky K, *et al*. (2016) Pulse and surge profiles of luteinizing hormone secretion in the mouse. *Endocrinology* 157(12):4794-4802.
21. Fergani C & Navarro VM (2017) Expanding the role of tachykinins in the neuroendocrine control of reproduction. *Reproduction* 153(1):R1-R14.
22. Clarkson J, *et al*. (2017) Definition of the hypothalamic GnRH pulse generator in mice. *Proceedings of the National Academy of Sciences* 114(47):E10216-E10223.
23. Han SY, McLennan T, Czieselsky K, & Herbison AE (2015) Selective optogenetic activation of arcuate kisspeptin neurons generates pulsatile luteinizing hormone secretion. *Proceedings of the National Academy of Sciences* 112(42):13109-13114.
24. Campos P & Herbison AE (2014) Optogenetic activation of GnRH neurons reveals minimal requirements for pulsatile luteinizing hormone secretion. *Proceedings of the National Academy of Sciences* 111(51):18387-18392.
25. Lin Y, *et al*. (2010) The role of the medial and central amygdala in stress-induced suppression of pulsatile LH secretion in female rats. *Endocrinology* 152(2):545-555.
26. Padilla SL, *et al*. (2017) AgRP to Kiss1 neuron signaling links nutritional state and fertility. *Proceedings of the National Academy of Sciences*:201621065.
27. Doedel EJ, *et al*. (2007) AUTO-07P: Continuation and bifurcation software for ordinary differential equations.
28. Toni T, Welch D, Strelkowa N, Ipsen A, & Stumpf MPH (2009) Approximate Bayesian computation scheme for parameter inference and model selection in dynamical systems. *Journal of The Royal Society Interface* 6(31):187-202.
29. Ruka KA, Burger LL, & Moenter SM (2015) Both Estrogen and Androgen Modify the Response to Activation of Neurokinin-3 and κ-Opioid Receptors in Arcuate Kisspeptin Neurons From Male Mice. *Endocrinology* 157(2):752-763.
30. Yasuda K, *et al*. (1993) Cloning and functional comparison of kappa and delta opioid receptors from mouse brain. *Proceedings of the National Academy of Sciences* 90(14):6736-6740.
31. Seabrook GR, Bowery BJ, & Hill RG (1995) Pharmacology of tachykinin receptors on neurones in the ventral tegmental area of rat brain slices. *European Journal of Pharmacology* 273(1-2):113-119.
32. Yeo SH, *et al*. (2016) Visualisation of Kiss1 Neurone Distribution Using a Kiss1-CRE Transgenic Mouse. *Journal of neuroendocrinology* 28(11).
33. Paxinos G & Franklin K (2004) The mouse brain in stereotaxic coordinates Amsterdam. (Boston, MA: Elsevier Academic Press).
34. Steyn FJ, *et al*. (2013) Development of a methodology for and assessment of pulsatile luteinizing hormone secretion in juvenile and adult male mice. *Endocrinology* 154(12):4939-4945.
35. Vidal A, Zhang Q, Médigue C, Fabre S, & Clément F (2012) DynPeak: An algorithm for pulse detection and frequency analysis in hormonal time series. *PLoS One* 7(7):e39001.